# The Beda Basalt: new geochemistry, isotopic data and its definition

*Claire E Wade, Stacey O McAvaney and Georgina A Gordon*
*Geological Survey of South Australia, Department of State Development*

*Peer reviewed (Department of State Development and externally)*

## Introduction

The Neoproterozoic Adelaide Geosyncline and Stuart Shelf preserve deposits formed in a major rift basin and shelf which now separate the Gawler and Curnamona provinces which developed during the break-up of the supercontinent Rodinia (Preiss 2000). The early stages of rifting and sedimentation were accompanied by localised basaltic and minor felsic magmatism within the basal Callanna Group, comprising the Wilangee Basalt near Broken Hill (NSW), the Cadlareena Volcanics in the Peake and Denison Inlier, the Noranda Volcanics in the Willouran Ranges, the Wooltana Volcanics bordering the Mount Painter Inlier, volcanics at Depot Creek in the southwest Flinders Ranges, the Boucaut Volcanics south of Olary, the Beda Basalt on the Stuart Shelf and the Gairdner Dolerite which intrudes the central Gawler Craton to the west; together these units have been referred to as the Willouran Basic Province (Fig. 1; Crawford and Hilyard 1990).

The Beda Basalt consists of a succession of subaerial, amygdaloidal to massive tholeiitic basalt flows interbedded with fluvial sandstones and conglomerates of the Backy Point Formation, which is exposed around the Cultana Inlier, an up-faulted block of the Gawler Craton on the northeast Eyre Peninsula, and occurs extensively in the subsurface within the Stuart Shelf (Figs 1, 2). This article provides new geochemical and isotopic data and a formal definition of the Beda Basalt (App. 1).

The basalts exposed around the Cultana Inlier (Fig. 2), which are here referred to as the Beda Basalt, were first mapped and described as the Roopena Volcanics, based on their petrological similarity with that sequence exposed south of Roopena Homestead ~40 km to the northwest (Crawford and Hiern 1964; Dalgarno et al. 1968; Crawford and Forbes 1969), which at the time

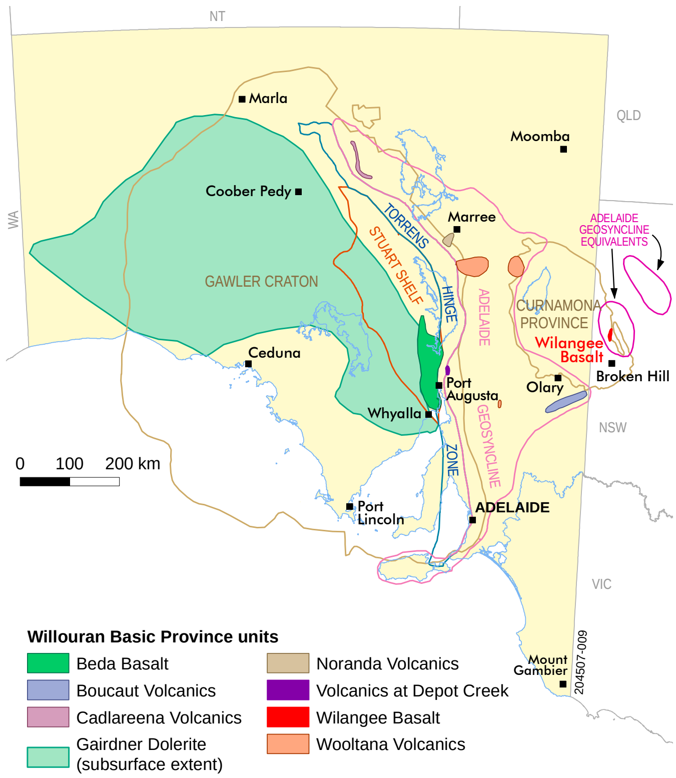


*Figure 1* *Map of Willouran Basic Province.*

were thought to be part of the Neoproterozoic Stuart Shelf sequence (Compston, Crawford and Bofinger 1966). They have since been recognised as belonging to the Mesoproterozoic Gawler Range Volcanics (Johnson 1993).

Subsequent drilling by Australian Selection Pty Ltd on the Stuart Shelf (Australian Selection 1977) revealed that the basalts exposed around the Cultana Inlier and the Roopena Volcanics to the northeast are not stratigraphically equivalent but separated by the Mesoproterozoic Pandurra Formation, and Mason,

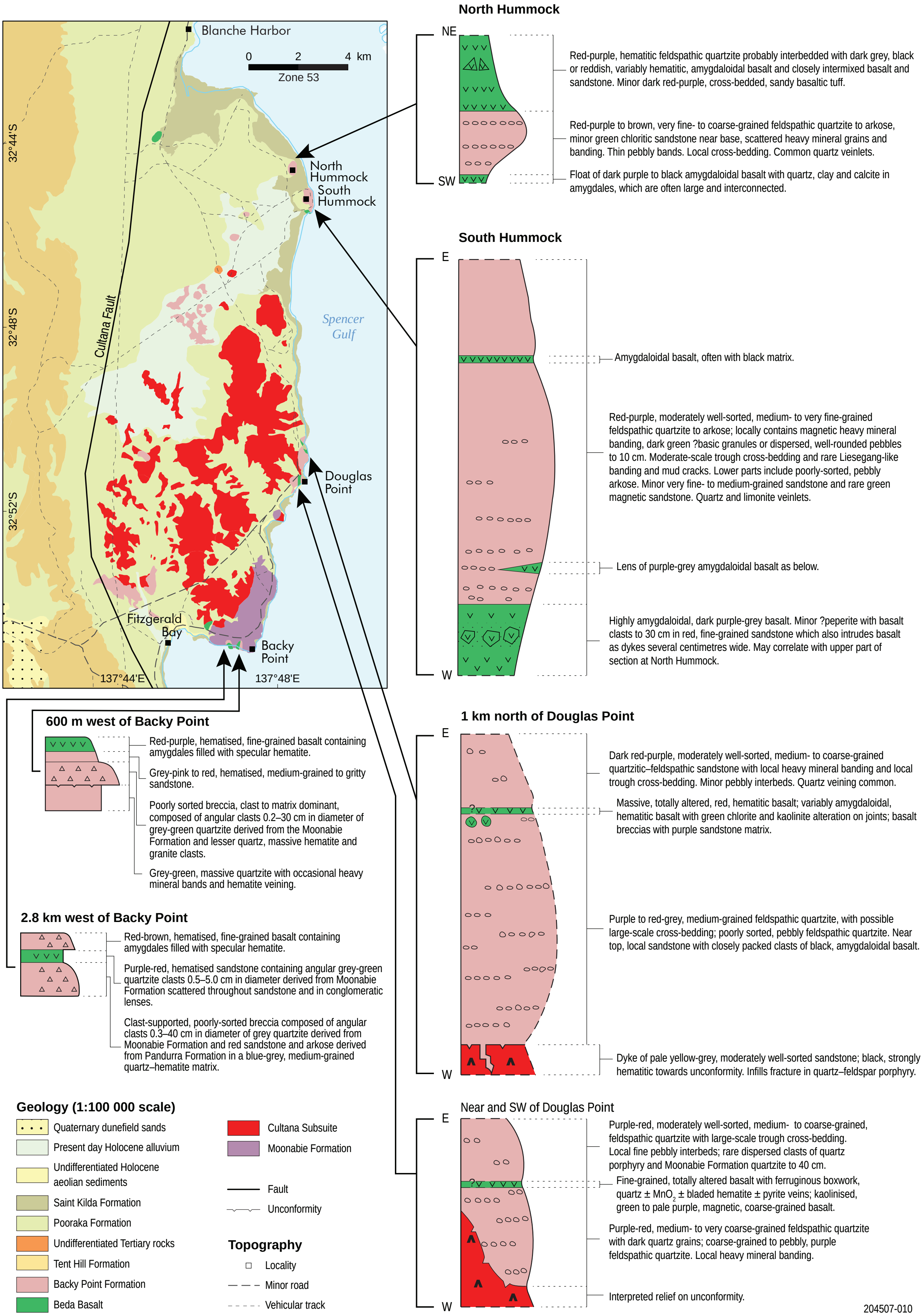


*Figure 2 Geology of the Beda Basalt and Backy Point Formation around the Cultana Inlier (adapted from Cowley 1991).*

Thomson and Tonkin (1978) were the first to use the name Beda Volcanics to describe the basalts overlying the Pandurra Formation in drillholes. While Mason, Thomson and Tonkin (1978) referred to the sediments as the Backy Point Beds, and Crawford and Forbes (1969) briefly defined these associated sediments as the Backy Point Formation, appearing on the PORT AUGUSTA 1:250 000 scale map, the authors never defined the Beda Volcanics due to an uncertainty about the relationship between what they termed the 'lower Beda Volcanics' which are interlayered with the Backy Point Formation and the thick basalt sequence of the 'upper spilitic flows', which are now accepted to be part of the same sequence.

Subsequent geochemical analysis of drillhole samples confirmed the distinction between the Beda Basalt and Roopena Volcanics (Giles and Teale 1979). The Beda Basalt has been compared lithologically and geochemically with a number of other basalt sequences in the Adelaide Geosyncline belonging to the c. 830 Ma Willouran Basic Province such as the Wooltana Volcanics, Cadlareena Volcanics, Noranda Volcanics, Wilangee Basalt, Boucaut Volcanics, volcanics at Depot Creek and the Gairdner Dolerite (Fig. 1; Preiss 1987; Woodget 1987; Hilyard 1989; Crawford and Hilyard 1990).

Most recently Cowley (1991) and Cowley and Flint (1993) described in greater detail the outcrop geology and drillhole stratigraphy of both the Beda Basalt and Backy Point Formation, inferring instead that they and the Gairdner Dyke Swarm (now Gairdner Dolerite) are Mesoproterozoic (c. 1076 Ma) and that the Gairdner Dolerite comprises feeder dykes to the basalts (Mason, Thomson and Tonkin 1978).

## Regional geological setting and stratigraphy

The Beda Basalt and Backy Point Formation are a sequence of interlayered fluvial sandstone and conglomerate and subaerial, amygdaloidal to massive tholeiitic basalt. The Beda Basalt occurs extensively beneath the cover of the younger Neoproterozoic units of the Stuart Shelf in a northwest-trending belt ~190 km by 40 km between the southern tip of the Cultana Inlier and the Carrapateena Arm of Lake Torrens (Fig. 3).

The only exposure of the formation occurs around the Cultana Inlier, a faulted block of the Gawler Craton which has undergone uplift along the Cultana Fault, removing the younger Neoproterozoic sequence and exposing the Beda Basalt along the coast of the northwestern Spencer Gulf near Backy Point, North and South Hummocks and north of Douglas Point (Fig. 2).

The type locality of the Beda Basalt is taken here as the exposures around the southeastern Cultana Inlier (Cowley 1991), including Douglas Point (GDA94, zone 53, 762970mE, 6361550mN, extending 400 m to the east and 1.7 km to the north) and 1 km ENE of Backy Point (extending 400 m around the point GDA94, 760060mE, 6354950mN; Fig. 2). These sites can be accessed by turning east along Port Bonython Road from the Lincoln Highway ~10 km north of Whyalla, and turning left after 16 km onto Fitzgerald Bay Road, which connects with a coastal track passing through Backy and Douglas points. Additional exposures at North Hummock (GDA94, zone 53, 762400mE, 6374060mN) and South Hummock (GDA94, zone 53, 763000mE, 6372800mN) lie within the Cultana Army Training Area and are not readily accessible, requiring negotiation with the Australian Defence Force.

The reference drillhole PSH 1/SAS 1 (SA Geodata Drillhole (DH) Number 136943; GDA94, 734729mE, 6409671mN), located 25 km west of Port Augusta (Fig. 3), within the interval 273.7–470.44 m is proposed. This hole was originally recommended as a reference drillhole by Mason, Thomson and Tonkin (1978) and here a new graphic log is provided (Fig. 4).

## Lithology

The Beda Basalt is a sequence of subaerial amygdaloidal to massive tholeiitic basalts (Fig. 5). Although intersected in over 100 drillholes, only 30 penetrate to the base of the sequence. The preserved thickness of the basalt is variable, ranging from 1.1 m in drillhole PUB 40/SAU 24 (DH Number 139504) to almost 550 m in BDH 3 (DH Number 25356; Fig. 3) which contains ~70 flows (Delhi Petroleum Pty Ltd, Urangesellschaft Australia Pty Ltd and CSR Ltd 1986). The true thickness of the Beda Basalt is uncertain, as it was exposed everywhere to subaerial weathering and erosion prior to the deposition of the Tapley Hill Formation in the early Sturtian.

The basalts are substantially altered (Fig. 5a), but primary igneous textures are well preserved. They are composed of sericitised and chloritised plagioclase laths in a hematised and chloritised matrix of coarse-grained, green-yellow clinopyroxene altered to actinolite, tremolite, chlorite and epidote and introduced potassium feldspar (Fig. 5b; Mason, Thomson and Tonkin 1978; Cowley 1991). Amygdales contain calcite, quartz, chlorite, specular hematite, potassium feldspar and albite (Figs 5b, c). Flows range in thickness from <1 m to ~30 m thick. Brecciated flow tops are only sporadically developed and flow margins are most commonly marked by red-brown, fine-grained to

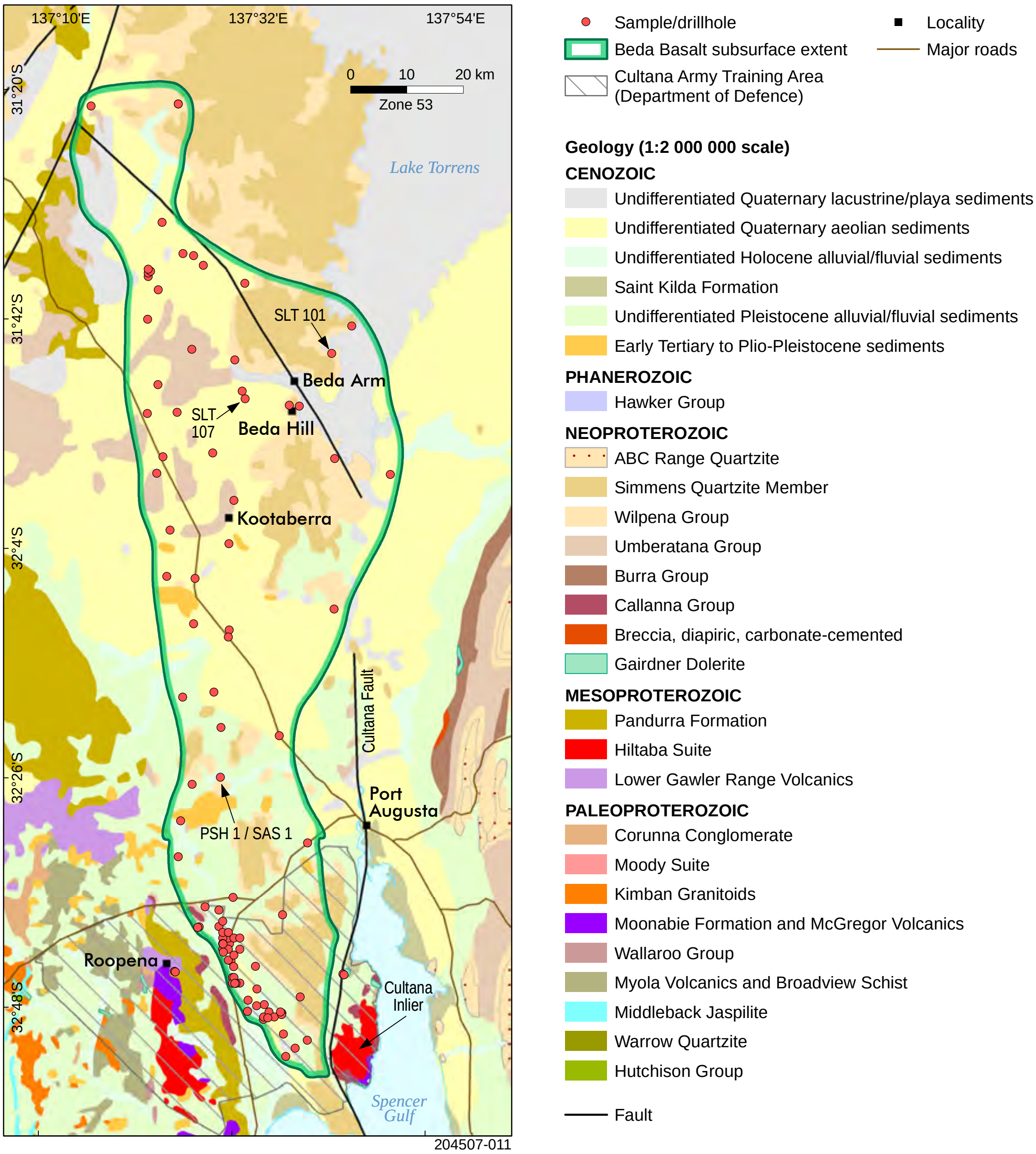


*Figure 3* *Subsurface extent of the Beda Basalt.*

aphanitic basalt containing small densely packed amygdales (Figs 5d, e). The middle of the flows, particularly the thicker ones, consist of grey-black, medium-grained basalt with larger sparsely packed amygdales (Figs 5d, f). Small lenses of sand or silt or larger sandstone and conglomerate beds of the Backy Point Formation are recorded between many flows (Figs 4, 5d).

The interval of Beda Basalt within reference drillhole PSH 1/SAS 1 consists of a pile of 22 lava flows ranging from <1 m to almost 30 m thick, totalling almost 200 m (Figs 3, 4). Thin (5–20 cm) red siltstone beds occur between some flows. Logged flows coincide with sharp changes in the visible short wave infrared (VSWIR) and thermal infrared (TIR) HyLogger$^{TM}$ spectra (Fig. 4), reflecting a difference in the bulk mineral composition of amygdaloidal-rich tops and pyroxene-rich bottoms of the basalt flows compared to the amygdaloidal-sparse flow middles (see Gordon et al. 2014, this volume).

The Beda Basalt is interlayered with the Backy Point Formation, a white, red to purple, fine- to coarse-grained feldspathic and lithic sandstone to conglomerate with minor interbeds of red, brown and green micaceous siltstone. Interlayering can be observed in outcrop at North and South Hummocks, Douglas Point and west of Backy Point (Fig. 6a). In drillhole intersections southwest of the Cultana Inlier the Beda Basalt is interbedded with intervals several metres thick of Backy Point Formation (e.g. TR 3, DH Number 20447; Fig. 6b), but to the east and north of here the sediments typically occur either underlying or overlying the basalt sequence, as thin (<10 cm) beds between flows or are absent altogether (Cowley 1991).

Sandstone is composed of subrounded to well-rounded quartz, feldspar and lithic grains. It is rich in iron oxides which define heavy mineral banding and contains accessory tourmaline, zircon and monazite (Cowley 1991). The matrix of the sandstone around the Cultana Inlier is composed of quartz overgrowths, whereas in drillhole intersections the matrix is typically hematitic or calcareous or locally sericitic. Trough cross-bedding is common, and indicates a fluvial depositional environment, with much of the detritus derived locally.

Conglomerate is composed of angular to well-rounded pebbles and cobbles of quartz, potassium feldspar, granite, quartz–feldspar porphyry and tourmaline–quartz rock derived from the Cultana Subsuite, felsic volcanics derived from the Gawler Range Volcanics, quartzite derived from the Pandurra and Moonabie formations and lesser chert, banded iron formation, hematite and gneiss (Cowley 1991).

At North and South Hummocks and north of Douglas Point the Backy Point Formation comprises basalt breccia composed of tightly packed angular clasts of amygdaloidal basalt in a sandstone matrix or an irregular mixture of basalt and sandstone with thin sandstone dykes intruding the basalt, and these are interpreted as volcanic bombs in sandstone or peperite (Fig. 6c; Cowley 1991).

Around the Cultana Inlier the Beda Basalt and Backy Point Formation unconformably overlie the Paleoproterozoic (c. 1745 Ma) Moonabie Formation (Fig. 6a) and Mesoproterozoic (c. 1585 Ma) Cultana Subsuite (McAvaney 2009), a porphyritic member of the Hiltaba Suite. On the Stuart Shelf they unconformably overlie the Pandurra Formation (Fig. 6e), and are typically unconformably overlain by the Tapley Hill Formation (Fig. 6f), the basal beds of which often contain clasts derived from the Beda Basalt.

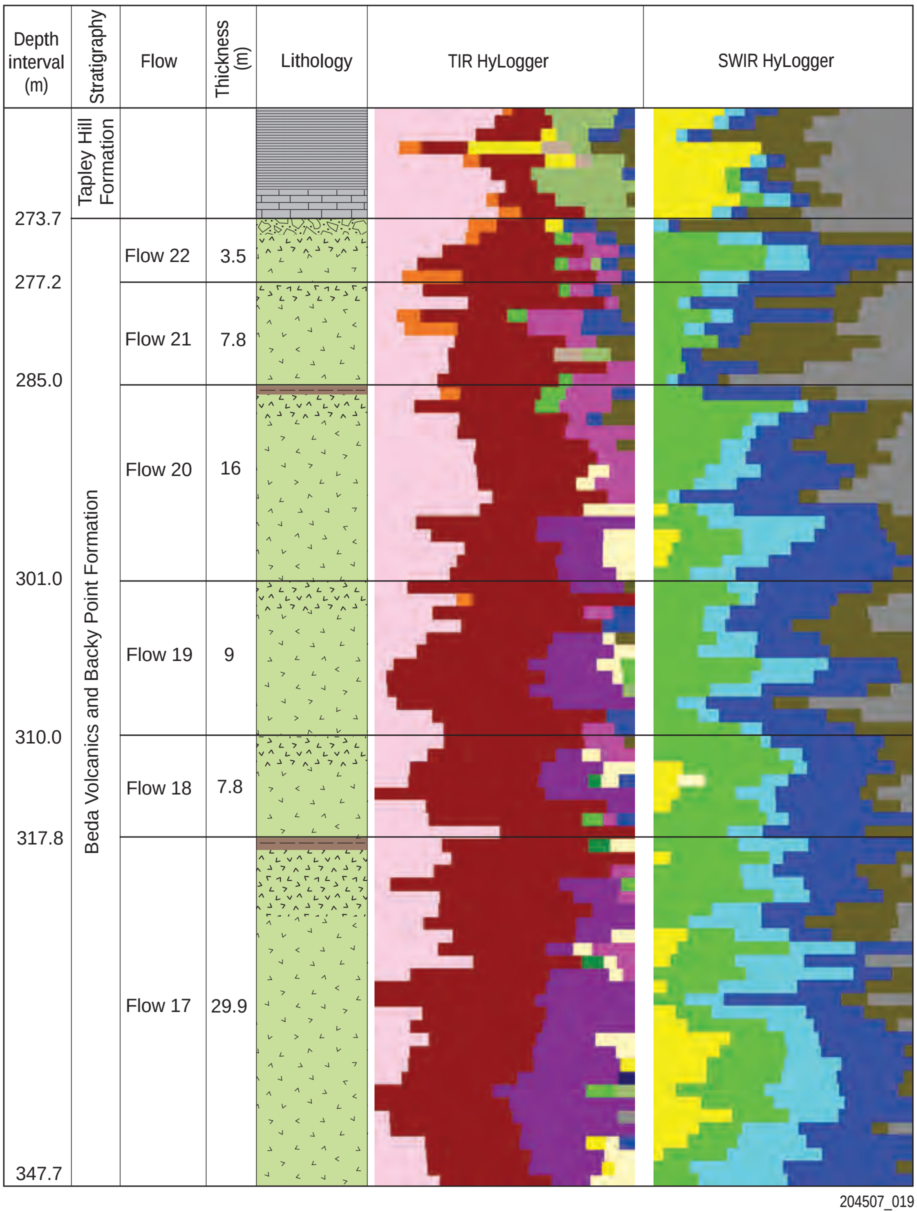


*Figure 4* Geological log of reference drillhole PSH 1/SAS 1 showing logged lava flows and HyLogger TIR and SWIR logs. See Gordon et al. 2014 (this volume) for discussion about HyLogger results and the mineralogical composition of the basalt flows.

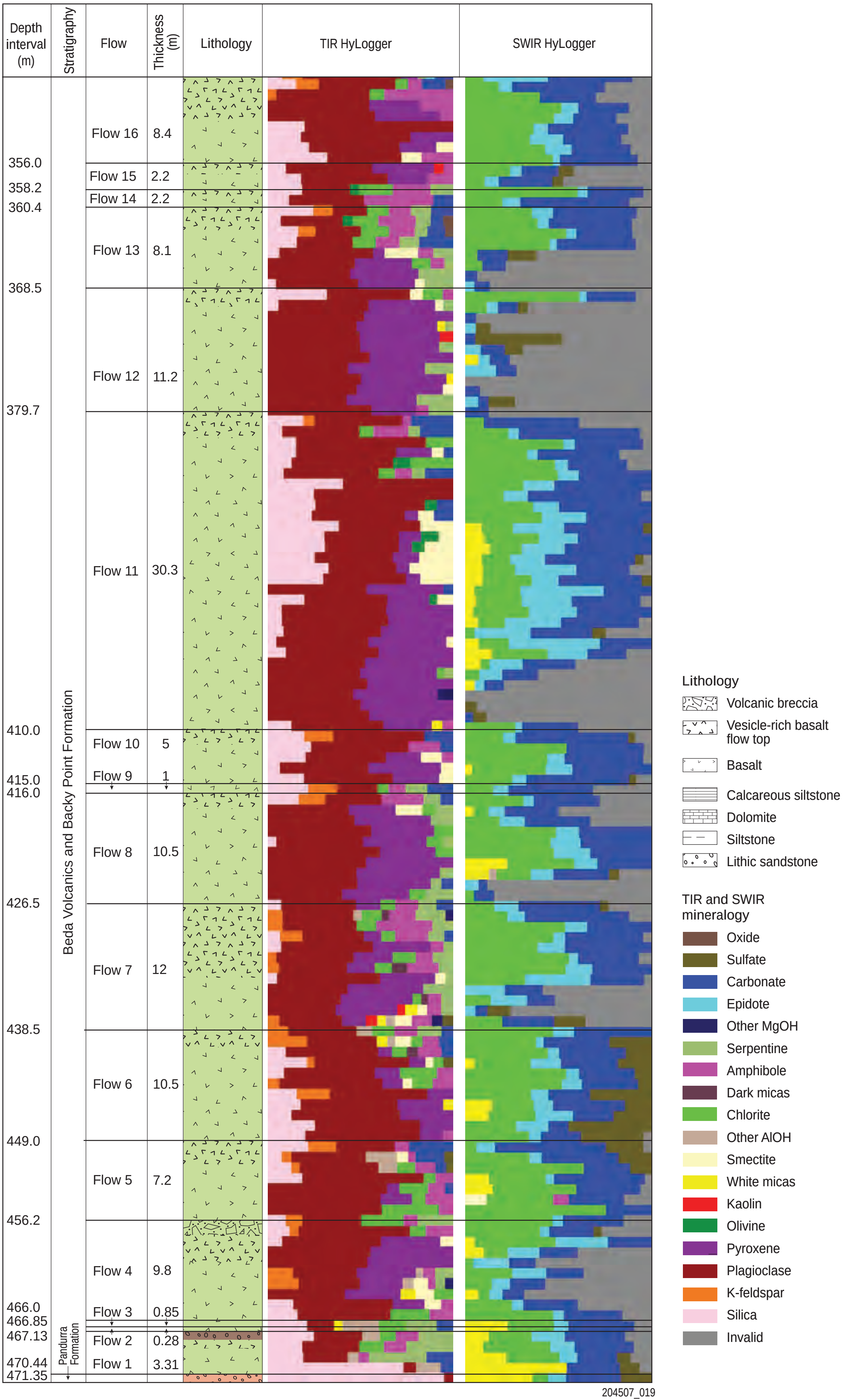

Depth interval (m)
Stratigraphy
Flow
Thickness (m)
Lithology
TIR HyLogger
SWIR HyLogger
356.0
358.2
360.4
368.5
379.7
410.0
415.0
416.0
426.5
438.5
449.0
456.2
466.0
466.85
467.13
470.44
471.35
Beda Volcanics and Backy Point Formation
Pandurra Formation
Flow 16
8.4
Flow 15
2.2
Flow 14
2.2
Flow 13
8.1
Flow 12
11.2
Flow 11
30.3
Flow 10
5
Flow 9
1
Flow 8
10.5
Flow 7
12
Flow 6
10.5
Flow 5
7.2
Flow 4
9.8
Flow 3
0.85
Flow 2
0.28
Flow 1
3.31
Lithology
Volcanic breccia
Vesicle-rich basalt flow top
Basalt
Calcareous siltstone
Dolomite
Siltstone
Lithic sandstone
TIR and SWIR mineralogy
Oxide
Sulfate
Carbonate
Epidote
Other MgOH
Serpentine
Amphibole
Dark micas
Chlorite
Other AlOH
Smectite
White micas
Kaolin
Olivine
Pyroxene
Plagioclase
K-feldspar
Silica
Invalid
204507_019

5 (a) Hematised basalt cropping out along shoreline 2.7 km WNW of Backy Point, looking east (site 1366487). (Photo 414075)

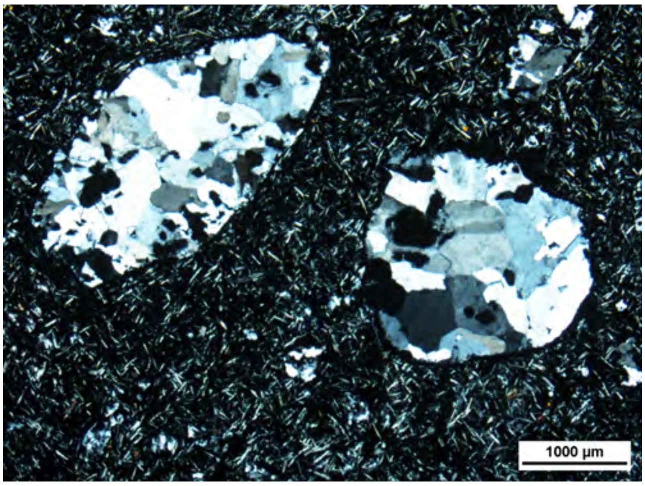


5 (b) Photomicrograph of basalt composed of quartz-filled amygdales and acicular plagioclase laths in a black, fine-grained groundmass (sample 1110471). (Photo 414076)

5 (c) Basalt containing potassium feldspar filled amygdales, South Hummock (site 1841183). (Photo 414077)


5 (d) Basalt flows in drillhole PSH 1/SAS 1. Flow 9 overlies sedimentary bed (s); flow 10 contains amygdalar top and bottom (a) and massive middle of flow (m). (Photo 414078)

5 (e) Red-brown, fine-grained amygdale-rich flow top, drillhole PSH 1/SAS 1. (Photo 414079)

5 (f) Grey-green, medium-grained basalt in middle of flow, drillhole PSH 1/SAS 1. (Photo 414080)

*Figure 5 Beda Basalt.*

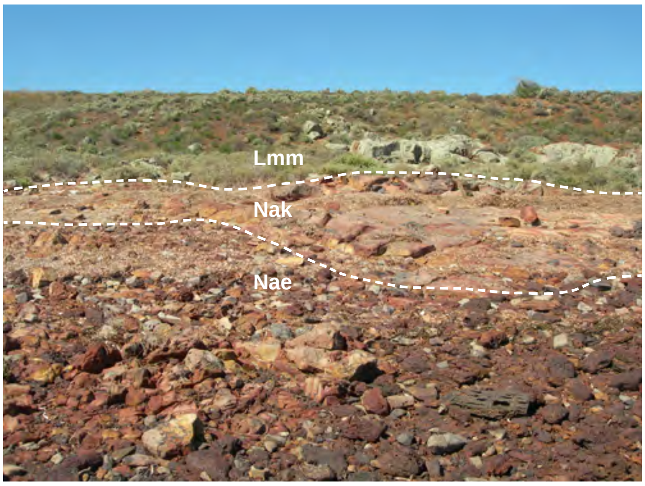


6 *(a) Beda Basalt (Nae) and pink sandstone of the Backy Point Formation (Nak) overlying the Moonabie Formation (Lmm). Site 1375584, 650 m west of Backy Point, looking north. (Photo 414081)*

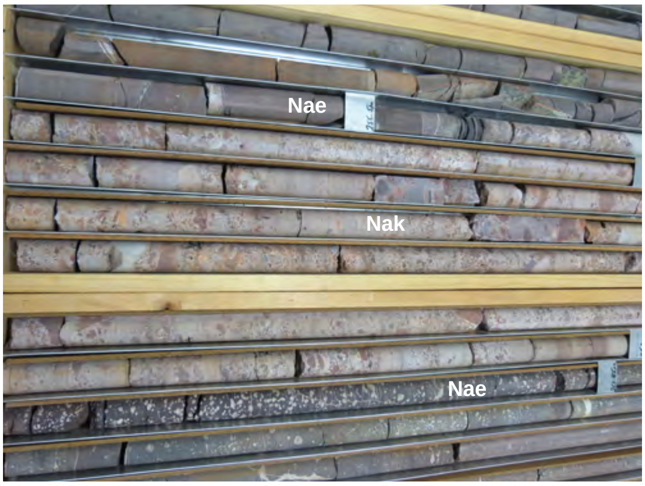


6 *(b) Purple sandstone and polymict conglomerate of the Backy Point Formation (Nak) interlayered with amygdaloidal and massive basalt of the Beda Basalt (Nae) in drillhole TR 3. (Photo 414082)*

6 *(c) Example of peperite in drillcore from drillhole BDH 2, ~550 m. (Photo 414083)*


6 *(d) Beda Basalt overlain by red siltstone of the Backy Point Formation containing basalt clasts in drillhole BDH 2. (Photo 414084)*

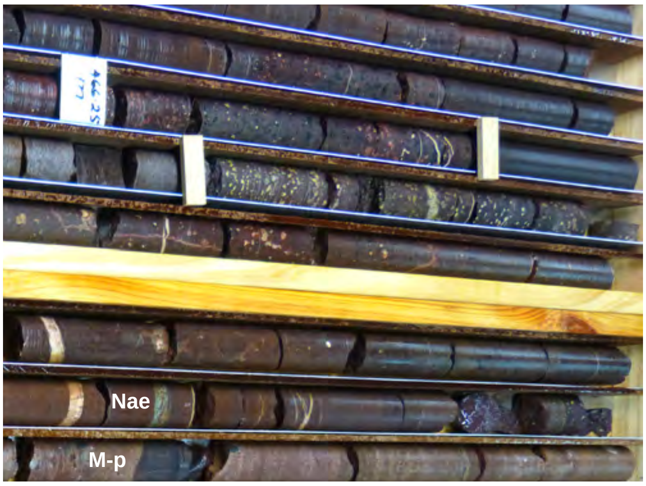


6 *(e) Beda Basalt (Nae) unconformably overlying red, pebbly sandstone of the Pandurra Formation (M-p) in drillhole PSH 1/SAS 1. (Photo 414085)*

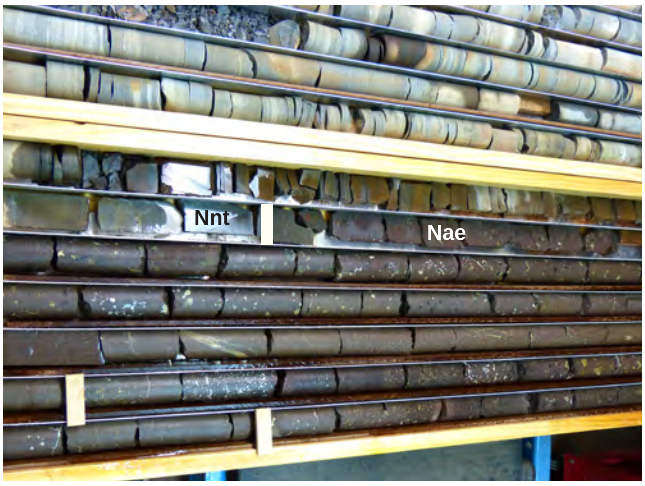


6 *(f) Beda Basalt (Nae) unconformably overlain by calcareous siltstone of the Tapley Hill Formation (Nnt) in drillhole PSH 1/SAS 1. (Photo 414086)*

*Figure 6 Contact relationships of the Beda Basalt.*

*Table 1* *New major and trace element data for the Beda Basalt*

| Sample | 1110471 | 1951542 | 1951543 | 1951544 | 1951545 | 1959427 | 1961524 | 1961525 | 1961526 |
|---|---|---|---|---|---|---|---|---|---|
| Lithology | Basalt | Basalt | Basalt | Basalt | Basalt | Basalt | Basalt | Basalt | Basalt |
| Easting (m) | 762554 | 729679 | 729679 | 729679 | 729679 | 743129 | 734799 | 734799 | 734799 |
| Northing (m) | 6374100 | 6408451 | 6408451 | 6408451 | 6408451 | 6367031 | 6418512 | 6418512 | 6418512 |
| Drillhole | | TR3 | TR3 | TR3 | TR3 | CU12 | TR6 | TR6 | TR6 |
| Depth from (m) | | 249.75 | 251.02 | 270.32 | 282.41 | 214.30 | 212.50 | 219.00 | 225.65 |
| Depth to (m) | | 250.10 | 251.58 | 270.90 | 282.95 | 214.58 | 212.85 | 219.35 | 226.07 |
| $SiO_2$ | 58.0 | 42.8 | 51.3 | 51.3 | 51.2 | 45.2 | 50.4 | 50.1 | 50.6 |
| $TiO_2$ | 1.0 | 1.8 | 1.9 | 1.3 | 1.4 | 2.2 | 1.8 | 1.7 | 1.7 |
| $Al_2O_3$ | 8.5 | 15.2 | 13.6 | 14.3 | 14.7 | 15.9 | 13.6 | 13.3 | 13.3 |
| $Fe_2O_3t$ | 26.6 | 12.6 | 14.1 | 12.1 | 13.6 | 14.7 | 14.0 | 14.1 | 13.9 |
| MnO | 0.0 | 0.8 | 0.2 | 0.2 | 0.3 | 1.9 | 0.2 | 0.2 | 0.2 |
| MgO | 0.2 | 9.9 | 6.9 | 10.6 | 9.0 | 4.3 | 7.3 | 7.3 | 8.7 |
| CaO | 0.1 | 8.8 | 8.2 | 4.8 | 2.7 | 7.0 | 8.2 | 7.6 | 5.9 |
| $Na_2O$ | 4.1 | 0.8 | 2.7 | 3.1 | 4.1 | 2.1 | 2.6 | 3.2 | 4.6 |
| $K_2O$ | 1.2 | 5.8 | 0.9 | 2.1 | 2.5 | 5.3 | 1.7 | 2.0 | 1.0 |
| $P_2O_5$ | 0.0 | 0.2 | 0.2 | 0.1 | 0.1 | 0.2 | 0.2 | 0.1 | 0.2 |
| LOI | 0.5 | 12.1 | 3.7 | 4.4 | 4.4 | 11.2 | 2.4 | 2.0 | 3.2 |
| **Total** without LOI† | **100.0** | **98.7** | **99.8** | **99.9** | **99.6** | **98.8** | **99.9** | **99.7** | **99.9** |
| | | | | | | | | | |
| Ti | 5 988.1 | 9 880.3 | 10 778.6 | 7 365.4 | 7 904.3 | 11 796.5 | 10 419.3 | 9 700.7 | 9 820.5 |
| V | 312.0 | 366.0 | 416.0 | 338.0 | 350.0 | 408.0 | 341.0 | 329.0 | 351.0 |
| Cr | 120.0 | 180.0 | 190.0 | 250.0 | 230.0 | 190.0 | 160.0 | 160.0 | 150.0 |
| Co | 17.0 | 43.8 | 49.6 | 50.6 | 48.0 | 82.2 | 46.9 | 45.7 | 48.1 |
| Ni | 46.0 | 119.0 | 107.0 | 125.0 | 126.0 | 190.0 | 92.0 | 90.0 | 89.0 |
| Cu | 22.0 | 19.0 | 75.0 | 53.0 | 49.0 | 115.0 | 61.0 | 48.0 | 60.0 |
| Zn | 54.0 | 78.0 | 112.0 | 142.0 | 190.0 | 54.0 | 121.0 | 114.0 | 136.0 |
| Pb | 12.0 | 10.0 | 15.0 | 31.0 | 23.0 | 7.0 | 13.0 | 15.0 | 21.0 |
| Ga | 8.7 | 18.3 | 19.1 | 16.8 | 17.0 | 20.8 | 18.2 | 17.8 | 17.8 |
| Cs | 0.3 | 3.4 | 3.5 | 3.2 | 2.1 | 5.7 | 2.0 | 4.4 | 1.2 |
| Rb | 39.3 | 202.0 | 34.1 | 84.8 | 87.8 | 270.0 | 84.8 | 98.5 | 41.1 |
| Ba | 94.7 | 264.0 | 148.0 | 327.0 | 414.0 | 197.5 | 197.0 | 389.0 | 123.0 |
| Sr | 22.3 | 38.5 | 148.5 | 117.5 | 130.0 | 22.0 | 144.0 | 146.5 | 111.5 |
| Y | 15.6 | 28.8 | 26.4 | 19.6 | 21.5 | 22.0 | 23.5 | 22.0 | 23.9 |
| Zr | 64.0 | 107.0 | 116.0 | 79.0 | 92.0 | 122.0 | 110.0 | 104.0 | 115.0 |
| Th | 1.9 | 2.3 | 1.8 | 1.6 | 2.5 | 1.8 | 1.6 | 1.4 | 2.0 |
| U | 6.2 | 1.8 | 0.3 | 0.3 | 0.9 | 1.5 | 0.4 | 0.3 | 0.4 |
| Nb | 4.7 | 6.8 | 7.4 | 4.8 | 5.4 | 8.3 | 7.0 | 6.5 | 7.3 |
| Ta | 0.4 | 0.5 | 0.5 | 0.4 | 0.4 | 0.6 | 0.5 | 0.5 | 0.5 |
| Hf | 2.0 | 3.1 | 3.3 | 2.3 | 2.6 | 3.5 | 3.1 | 2.9 | 3.2 |
| | | | | | | | | | |
| La | 6.1 | 13.6 | 10.7 | 7.9 | 9.7 | 17.3 | 10.1 | 9.6 | 11.0 |
| Ce | 18.8 | 32.9 | 24.0 | 16.9 | 20.7 | 45.4 | 22.4 | 20.9 | 24.0 |
| Pr | 2.4 | 5.0 | 3.6 | 2.5 | 3.2 | 7.0 | 3.1 | 2.8 | 3.3 |
| Nd | 10.8 | 22.7 | 16.4 | 11.6 | 14.1 | 30.4 | 14.3 | 13.7 | 15.3 |
| Sm | 2.9 | 5.5 | 4.4 | 3.1 | 3.6 | 6.2 | 3.8 | 3.6 | 3.9 |
| Eu | 1.0 | 1.9 | 1.6 | 1.1 | 1.3 | 2.1 | 1.4 | 1.2 | 1.2 |
| Gd | 3.3 | 6.3 | 5.1 | 3.7 | 4.3 | 5.4 | 4.3 | 4.1 | 4.2 |
| Tb | 0.5 | 0.9 | 0.8 | 0.6 | 0.7 | 0.8 | 0.7 | 0.7 | 0.8 |
| Dy | 3.0 | 5.7 | 5.3 | 3.8 | 4.4 | 4.7 | 4.5 | 4.4 | 4.5 |
| Ho | 0.6 | 1.1 | 1.0 | 0.8 | 0.9 | 0.9 | 0.9 | 0.8 | 0.9 |
| Er | 1.6 | 3.0 | 3.0 | 2.3 | 2.5 | 2.7 | 2.5 | 2.5 | 2.7 |
| Tm | 0.2 | 0.4 | 0.4 | 0.3 | 0.4 | 0.4 | 0.4 | 0.4 | 0.4 |
| Yb | 1.5 | 2.5 | 2.5 | 1.9 | 2.1 | 2.5 | 2.3 | 2.2 | 2.4 |
| Lu | 0.2 | 0.4 | 0.4 | 0.3 | 0.3 | 0.4 | 0.4 | 0.3 | 0.4 |
| | | | | | | | | | |
| Eu/Eu* | 1.0 | 1.0 | 1.0 | 1.0 | 1.0 | 1.1 | 1.0 | 1.0 | 0.9 |
| Zr/Y | 4.1 | 3.7 | 4.4 | 4.0 | 4.3 | 5.5 | 4.7 | 4.7 | 4.8 |
| Nb/Y | 0.3 | 0.2 | 0.3 | 0.2 | 0.3 | 0.4 | 0.3 | 0.3 | 0.3 |
| Zr/Nb | 13.6 | 15.7 | 15.7 | 16.5 | 17.0 | 14.7 | 15.7 | 16.0 | 15.8 |
| Ti/V | 19.2 | 27.0 | 25.9 | 21.8 | 22.6 | 28.9 | 30.6 | 29.5 | 28.0 |
| $(La/Yb)_N$ | 3.0 | 4.0 | 3.1 | 2.9 | 3.3 | 5.0 | 3.1 | 3.2 | 3.3 |

† Major element values normalised to LOI-free assuming 100% totals.

LOI = loss on ignition.

$Eu/Eu^* = EuN/(SmN \times GdN)^{0.5}$

## Geochronology

The age of the Beda Basalt is not well constrained due to its unsuitability for U–Pb dating and the fact that it is bound above and below by a lengthy hiatus. The youngest U–Pb zircon maximum depositional age obtained for the underlying Pandurra Formation is 1575 ± 5 Ma for a sample from Red Rock Hill on the northeast Eyre Peninsula (Fraser and Neumann 2010). Rb–Sr analyses of siltstone and shale beds from the Pandurra Formation in drillholes Peeweena 1 (DH Number 16698; incorrectly called Red Millers Creek 1) and PY 1 (DH Number 20712) gave a date of 1424 ± 51 Ma, interpreted as a maximum depositional age (Fanning, Flint and Preiss 1983). Samples of the basal Tindelpina Shale Member of the overlying Tapley Hill Formation from drillholes Blinman 2 (DH Number 69427) in the Adelaide Geosyncline and SCYW-79 1A (DH Number 20829) on the Stuart Shelf yield a combined Re–Os age of 643 ± 2.4 Ma (Kendall, Creaser and Selby 2006).

Direct Rb–Sr and Ar–Ar geochronology have yielded conflicting results for the Beda Basalt. Webb and Hörr (1978) obtained a whole rock Rb–Sr age of 697 ± 34 Ma from an amygdaloidal flow in drillhole PSH 1/SAS 1. Webb and Coats (1980) obtained a Rb–Sr age of 1076 ± 34 Ma for an altered basalt from drillhole Delhi–Aquitane BDH 2 (DH Number 25355) located 8 km west of Beda Hill on the southwestern edge of Lake Torrens (Fig. 3). Page, McCulloch and Black (1984) reprocessed the age obtained by Webb and Coats (1980) by removing samples with the greatest degree of alteration from the isochron, and obtained an age of c. 1200 Ma. The Beda Basalt is now generally accepted as belonging to the Willouran Basic Province based on its geochemical affinity to other volcanics within the province (Woodget 1987; Crawford and Hilyard 1990) which are constrained by geochronology to c. 830 Ma (Compston, Crawford and Bofinger 1966; Zhao, McCulloch and Korsch 1994; Wingate et al. 1998). Furthermore, Wingate et al. (1998) report an 827 ± 7 Ma Pb–Pb baddeleyite age for the Gairdner Dolerite, interpreted as feeders to the Beda Basalt.

Additional constraint on the age of the Beda Basalt is provided by the U–Pb zircon age of 802 ± 10 Ma (Fanning et al. 1986) for the Rook Tuff in the Willouran Ranges, within the Curdimurka Subgroup, younger than the Arkaroola Subgroup which contains the Wooltana Volcanics, correlated with the Beda Basalt.

## Geochemistry

The Beda Basalt is classified as subalkaline basalt to trachybasalt, basaltic trachyandesite, basaltic andesite and andesite (Figs 7a, b). The Beda Basalt displays both tholeiitic and calcalkaline affinity on the AFM classification diagram (Fig. 7c). The ternary Ti + Fe – Al–Mg diagram classifies the Beda Basalt as high-Fe and high-Mg tholeiitic basalt (Fig. 7d). Basalts classified as high-Fe tholeiites have likely been affected by ferruginisation.

Beda Basalt has a broad range of silica content (42.83–58.2%; Table 1). MgO content is also variable (0.2–13%; typically 3–13%; Table 1). Beda Basalt is characterised by low $K_2O$ (<6%), high CaO (typically 3.8–≥11%) and high $Na_2O$ (typically 2.1–7.4%; Table 1; Fig. 8). Negative correlations are observed for CaO, $SiO_2$, $Na_2O$, $P_2O_5$, $Fe_2O_3$t and $TiO_2$ with increasing MgO; $Al_2O_3$ forms a positive correlation with increasing MgO (Fig. 8). High $Fe_2O_3$t co ntent is observed in a few samples (e.g. 1110471) and is likely attributed to ferruginisation. Major element abundances are similar to the Wooltana Volcanics (830 Ma basalts, northern Flinders Ranges) and the Gairdner Dolerite (827 Ma; Fig. 8). The Beda Basalt can be more enriched in $P_2O_5$ and $TiO_2$ compared with the Wooltana Volcanics (Fig. 8). Variation is observed in mobile elements such as CaO and $K_2O$, which are likely attributed to alteration. Compared with the basalts from Depot Creek, the Beda Basalt is enriched in CaO and displays less variation in major elements with increasing MgO (Fig. 8).

Beda Basalt displays similar trace element abundances to the Gairdner Dolerite and Wooltana Volcanics (Fig. 9). Enrichments in elements such as La, Ce, Nb and Zr are observed in the Beda Basalt compared to mafic rocks with similar MgO content (Fig. 9). While some scatter is observed in these elements (La, Ce, Zr and Nb), the data generally forms decreasing fractionation trends with increasing MgO content (Fig. 9). These trends are also observed in the Wooltana Volcanics and Gairdner Dolerite (Fig. 9). Beda Basalt displays some scatter in the large-ion lithophile elements (LILE, such as Rb, Ba, K and Sr) and mobile elements on primitive mantle-normalised trace element plots which is likely due to alteration. High field strength elements (HFSE, such as Th, U, Nb, Ta, Zr, and rare earth elements, REE) and immobile elements are relatively flat and close to enriched mid-ocean-ridge basalt (MORB) abundances (Fig. 10a). Some Beda Basalt samples display significant negative Sr anomalies indicating the fractionation of plagioclase, but this is not reflected in Eu depletions on REE plots (Fig. 10b). Trace element abundances are also compared with Wooltana Volcanics, basalts from Depot Creek and Gairdner Dolerite samples. Trace element patterns are indistinguishable from those of the Wooltana Volcanics and basalts from Depot Creek (Fig. 10a). While the Gairdner Dolerite displays more variation in trace elements, on Figure 10b the Beda Basalt generally fits within this field with the exception of Sr.

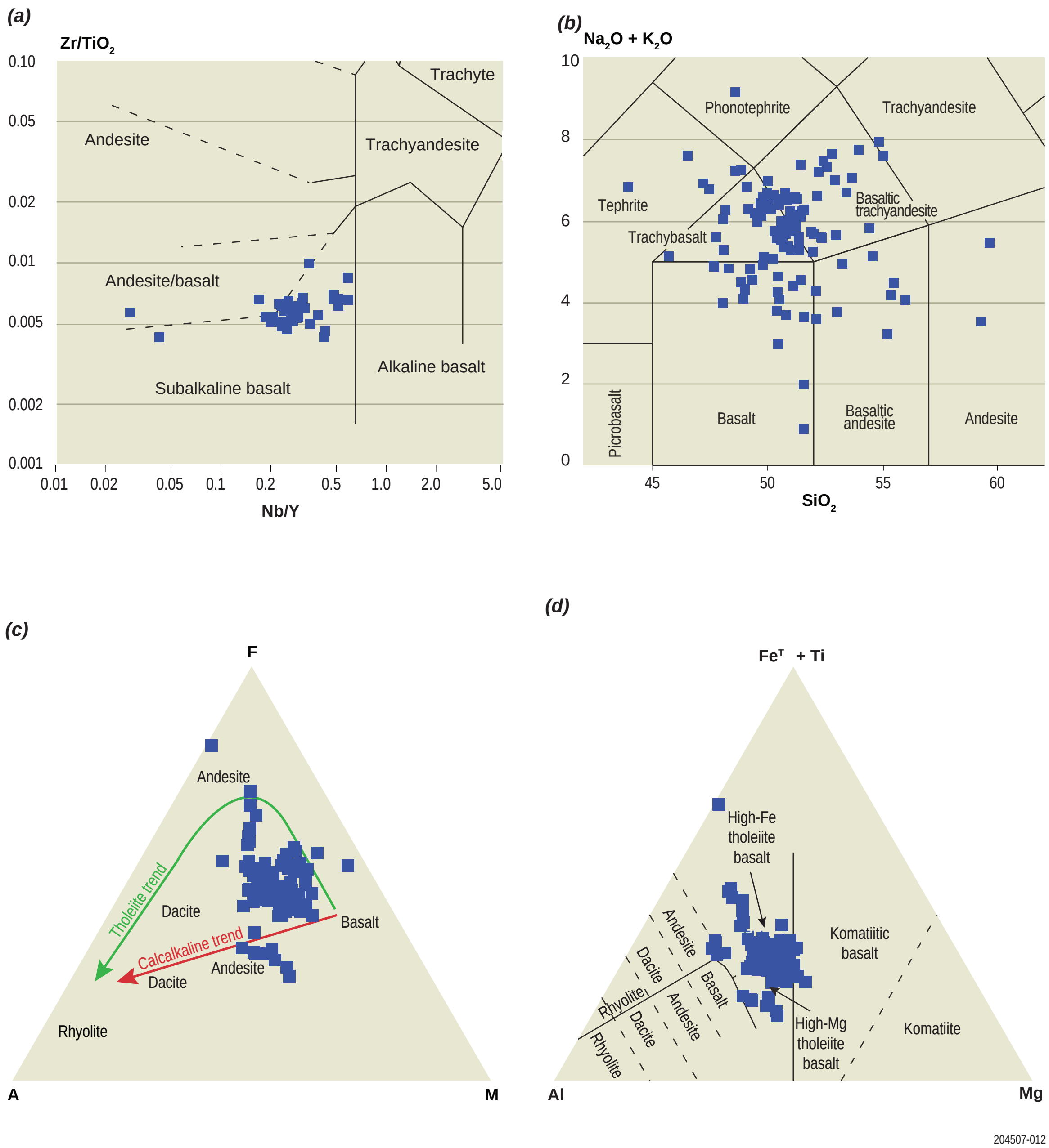


*Figure 7* *Classification diagrams for the Beda Basalt.* ***(a)*** *$Zr/TiO_2$–Nb/Y classification diagram (Floyd and Winchester 1978).* ***(b)*** *$Na_2O + K_2O – SiO_2$ diagram (Le Maitre et al. 1989).* ***(c)*** *AFM diagram (Kuno 1968; A = oxides of $Na_2O + K_2O$, F = oxides of $FeO + Fe_2O_3$ and M = oxides of MgO).* ***(d)*** *Ti + Fe – Al–Mg classification diagram (Jensen 1976).*

*Table 2* *Radiogenic isotope data for the Beda Basalt*

| **Sample** | **Lithology** | **Age** (Ma) | **Nd** (ppm) | **Sm** (ppm) | $^{147}Sm/^{144}Nd$ | $^{143}Nd/^{144}Nd$ | $T_{(DM)}$ | $T_{(CHUR)}$ | $\varepsilon Nd_{(0)}$ | $\varepsilon Nd_{(t)}$ |
|---|---|---|---|---|---|---|---|---|---|---|
| 1110471 | Basalt | 830 | 9.92 | 2.66 | 0.1622 | 0.512154 | 2.91 | 2.14 | –9.4 | –5.8 |
| 1951542 | Basalt | 830 | 21.74 | 5.50 | 0.1529 | 0.512265 | 2.20 | 1.30 | –7.3 | –2.6 |
| 1951544 | Basalt | 830 | 11.49 | 3.15 | 0.1659 | 0.512508 | 2.04 | 0.65 | –2.5 | 0.7 |
| 1959427 | Basalt | 830 | 27.44 | 5.76 | 0.1270 | 0.512328 | 1.45 | 0.68 | –6.0 | 1.3 |
| 1961524 | Basalt | 830 | 15.31 | 4.12 | 0.1626 | 0.512524 | 1.86 | 0.51 | –2.2 | 1.4 |
| 1961525 | Basalt | 830 | 14.70 | 3.97 | 0.1634 | 0.512553 | 1.81 | 0.39 | –1.7 | 1.9 |

Isotope error measurements are two times the standard error.
$^{143}Nd/^{144}Nd$ $CHUR_{(0)}$ = 0.512638; $^{147}Sm/^{144}Nd$ $CHUR_{(0)}$ = 0.1967; $^{143}Nd/^{144}Nd$ $DM_{(0)}$ = 0.51316; $^{147}Sm/^{144}Nd$ $DM_{(0)}$ = 0.2145
$T_{DM}$ =depleted-mantle model age; $T_{CHUR}$ = CHUR-model age.

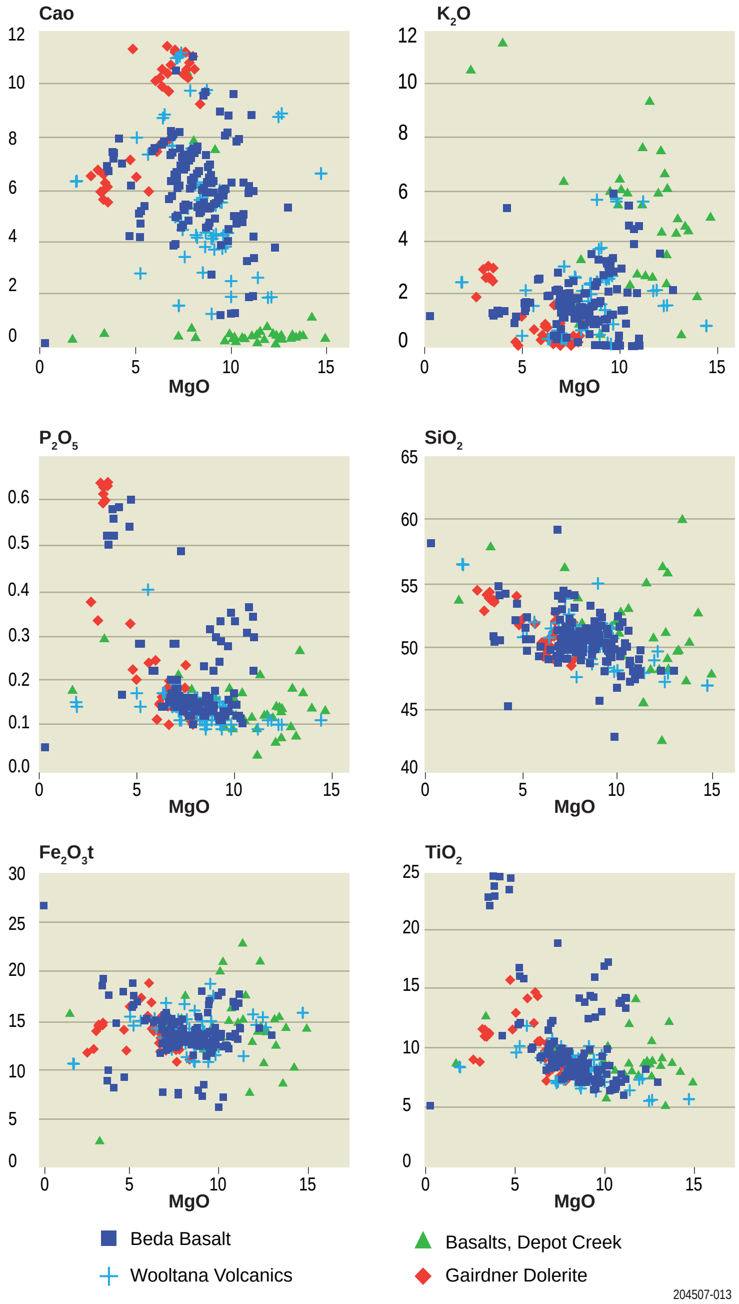


*Figure 8* *Major element variation diagrams for the Beda Basalt, Wooltana Volcanics, basalts from Depot Creek and Gairdner Dolerite.*

Beda Basalt displays REE profiles that are near flat with slight enrichment in light REE (LREE) relative to heavy REE (HREE; Fig. 10b), also indicated by low (La/YbN) ratios (2.9–5; where N represents values normalised to chondrite). Eu/Eu* values range from 0.9–1.1, which correspond to near-flat Eu anomalies (Table 1; Fig. 10b). LREE abundances for the Beda Basalt are variable and abundances range between enriched MORB and bulk crust values, while HREE abundances are more uniform and correspond to oceanic-island basalt, enriched MORB and bulk crust values (Fig. 10b). Beda Basalt is more enriched in LREE (La through to Gd) compared with the Wooltana Volcanics and basalts from Depot Creek, while HREE (Tb through to Lu) abundances are similar (Fig. 10b). REE abundances in the Beda Basalt display more overlap with the Gairdner Dolerite (Fig. 10b).

One outcrop and five drillhole Beda Basalt samples were analysed for whole-rock Sm–Nd analyses. These Sm–Nd results are listed in Table 2. $^{143}Nd/^{144}Nd$ values range from 0.512154–0.512553 and $^{147}Sm/^{144}Nd$ values between 0.1270 and 0.1659 (Table 2). These values are significantly lower than those reported by Foden et al. (2002) for the Beda Basalt ($^{143}Nd/^{144}Nd$ = 0.512707–0.512714 and $^{147}Sm/^{144}Nd$ = 0.1772–0.186) but comparable with Sm–Nd values of the volcanics at Depot Creek (Fig. 11). Beda Basalt samples with juvenile Nd signatures have $^{147}Sm/^{144}Nd$ ratios that are indistinguishable from the Gairdner Dolerite and Wooltana Volcanics. $T_{DM}$ values range from 1.4 to 2.9 Ga but form three $T_{DM}$ groups: ≤ 1.5 Ga, 1.6–2.1 Ga and ≥ 2.2 Ga. $\varepsilon_{Nd(830\ Ma)}$ values range from 5.8 to 3.4 (Table 2; Fig. 11). However, the Nd values for the Beda Basalt do not display any correlation with the $T_{DM}$ groups. While the Beda Basalt samples with the oldest $T_{DM}$ ages do have the most evolved Nd signatures, one sample with a $T_{DM}$ of 2.4 Ga has an $\varepsilon_{Nd(830\ Ma)}$ value of +2.6. Beda Basalt samples with $T_{DM}$ between 1.6 and 2.2 Ga have $\varepsilon_{Nd(830\ Ma)}$ values that range between 0.7 and 3.4 (Table 2). The sample with the youngest $T_{DM}$ (1.4 Ga) has an $\varepsilon_{Nd(830\ Ma)}$ value of +1.3. The majority of the Beda Basalt samples have $T_{DM}$ ages that are similar to the range for other Neoproterozoic mafic rocks (Foden et al. 2002), clustering around 1.6 Ga. At least two source regions appear to have been sampled during this event, an enriched mantle and a depleted mantle source, and more evolved signatures suggest assimilation of crustal material, most likely Mesoproterozoic basement either en route via crustal contamination or assimilation and fractional crystallisation (Fig. 11).

## Tectonic setting and source region discrimination

Figure 12 illustrates tectonic setting discrimination diagrams for basalts to distinguish within-plate basalts, island arc tholeiites and calcalkali basalts (Figs 12a, b); tholeiitic and alkali basalts (Figs 12c, d); and continental and oceanic tholeiites (Figs 12e, f).

Beda Basalt is a within-plate basalt as illustrated by the Ti–Zr–Y ternary diagram and the Zr/Y–Zr diagram (Figs 12a, b). Some overlap is observed between the within-plate basalt and MORB fields on these diagrams.

The Beda Basalt is predominantly continental tholeiite transitional to MORB as illustrated by the Ti/Y–Nb/Y diagram and $TiO_2$–Y/Nb (Figs 12c, d).

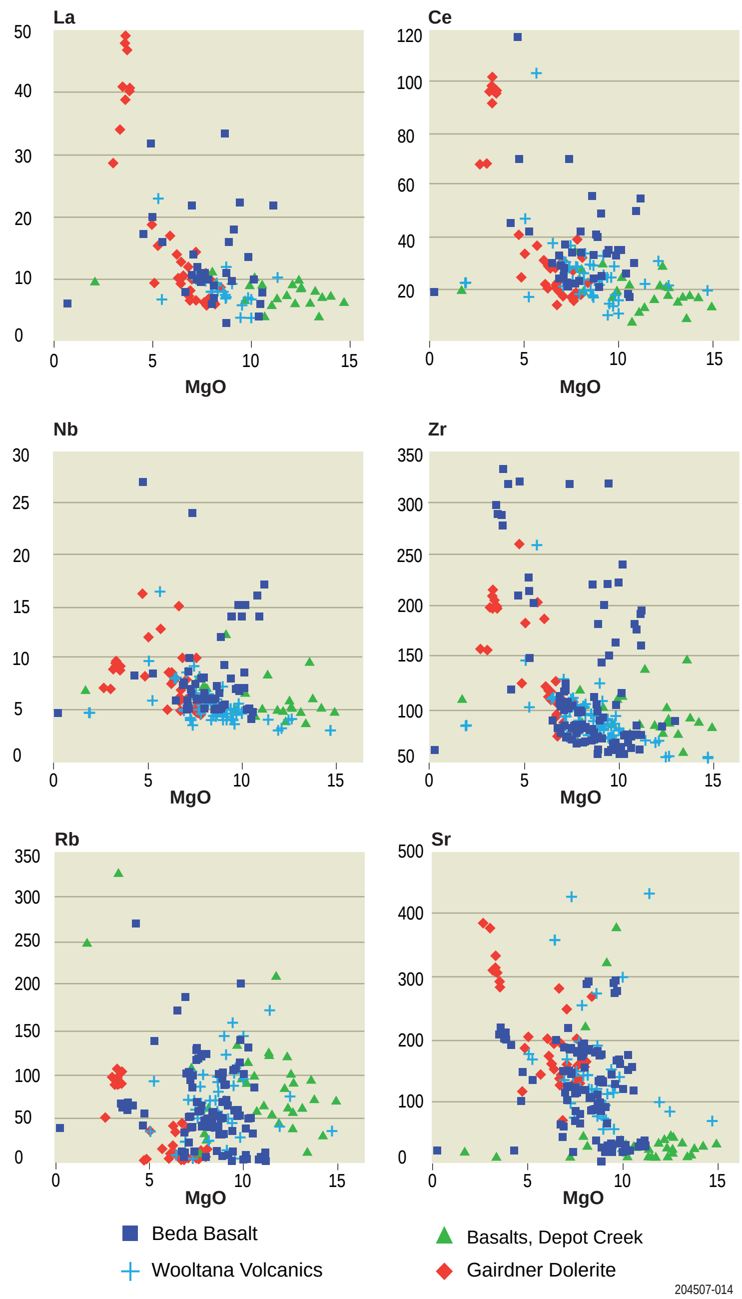


*Figure 9* Trace element variation diagrams for the Beda Basalt, Wooltana Volcanics, basalts from Depot Creek and Gairdner Dolerite.

Some samples from the Beda Basalt display oceanic affinity (Figs 12e, f).

Potential source regions for the Beda Basalt are shown on Figures 13a and 13b. On the Nb/Y–Zr/Y diagram the Beda Basalt lies on a trend between normal MORB or primitive mantle and crustal values, suggesting assimilation of lower to upper crustal material occurred either en route, or at some point prior to eruption, i.e. crustal contamination. Enriched LREE and trace element ratios such as La/Yb, Th/Nb, Ce/Y, Th/Sm, Zr/Y and Nb/Y are suggestive of crustal contamination, while Nb/La, Zr/Nb and La/Sm ratios and positive Nd values do not reflect significant amounts of assimilated crustal material (Fig. 13b).

While samples 1951542 and 1110471 have evolved Nd signatures, trace element ratios such as Zr/Y, Nd/Sm and Zr/Nb are similar to Beda Basalt with juvenile Nd signatures, enriched MORB and primitive mantle values, suggesting minor crustal contamination in conjunction with subcrustal alteration possibly occurred in these two samples. Incompatible element ratios are similar to enriched MORB values, while Nb/Zr ratios for all samples are indistinguishable from bulk crustal values and small negative Nb anomalies suggest small portions of crustal material may have been assimilated in the Beda Basalt.

## Implications for a large igneous province

The Willouran Basic Province in the base of the Adelaide Geosyncline sedimentary succession was first defined by Crawford and Hilyard (1990). This basic province included the following units: Wooltana Volcanics, Beda Basalt, Cadlareena Volcanics, Noranda Volcanics, Wilangee Basalt (Broken Hill) and the intrusive units, the Gairdner Dolerite and Little Broken Hill Gabbro (NSW). Further to this, additional Neoproterozoic-aged igneous rocks have also been identified as displaying geochemical affinity to the rocks from the Willouran Basic Province. These include the volcanics at Depot Creek, volcanics in Bitter Springs Formation (Amadeus Basin), pillow basalts in the Benagerie Ridge, Curnamona Province (LNM 10, DH Number 145894), and mafic volcanic and plutonic rocks in southern China (Zhao, McCulloch and Korsch 1994; Li et al. 1999; Wang et al. 2010).

Previous authors (Crawford and Hilyard 1990; Li et al. 1999; Wang et al. 2010), have discussed the significance of the Willouran Basic Province or large igneous province. It extends across more than 1000 km in south-central Australia and covers an area in excess of 210 000 $km^2$ (Crawford and Hilyard 1990). This prominent Neoproterozoic large igneous province is related to the breakup of the supercontinent Rodinia (Zhao, McCulloch and Korsch 1994; Li et al. 1999; Wang et al. 2010).

Mafic dyke swarms of the Gairdner Dolerite are interpreted as being derived from decompressional melting of a large-scale, uniform asthenospheric mantle plume. Flood basalt volcanism then followed as a result of the upwelling plume head causing doming in the continental lithosphere (Zhao, McCulloch and Korsch 1994) which produced the volcanics listed above, and including the Beda Basalt. The Gairdner Dolerite and other intrusive units are believed to be the feeders for the volcanics.

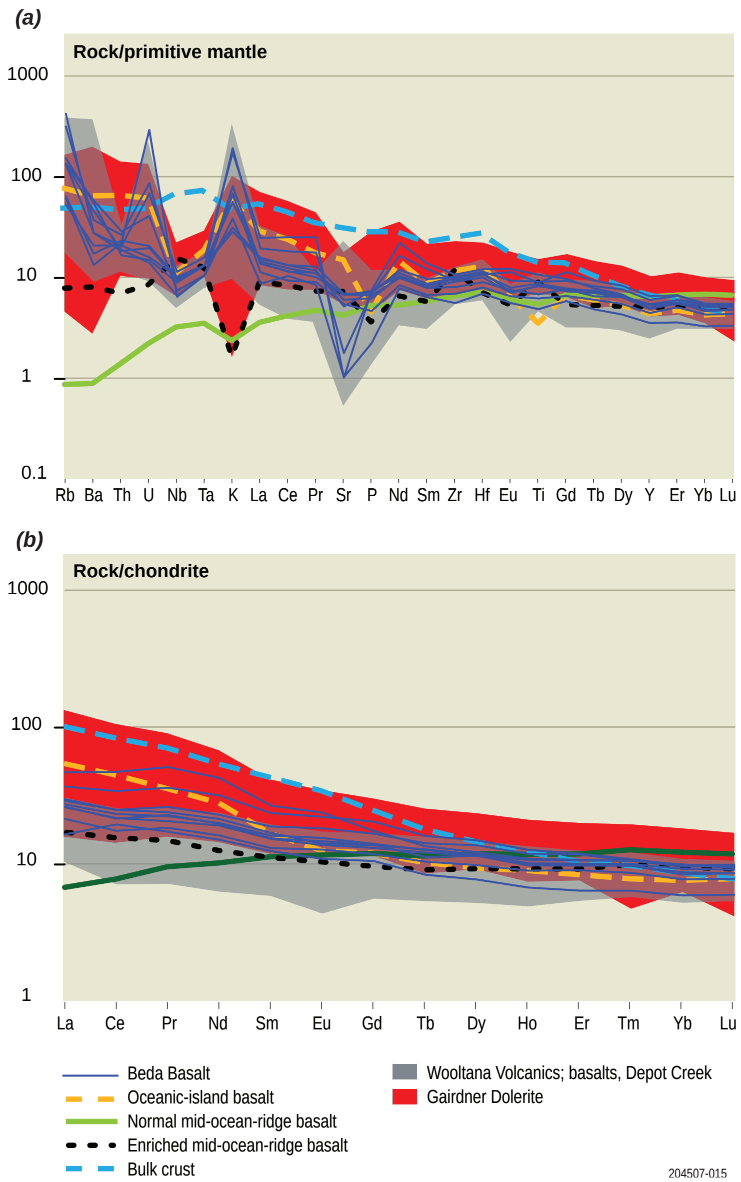


*Figure 10 Trace element (a) and REE data (b) for the Beda Basalt compared to Wooltana Volcanics, basalts from Depot Creek, Gairdner Dolerite, oceanic-island basalt (Sun and McDonough 1989), normal MORB (Hart et al. 1999), enriched MORB (Klein 2004) and bulk crust (Rudnick and Gao 2003).*

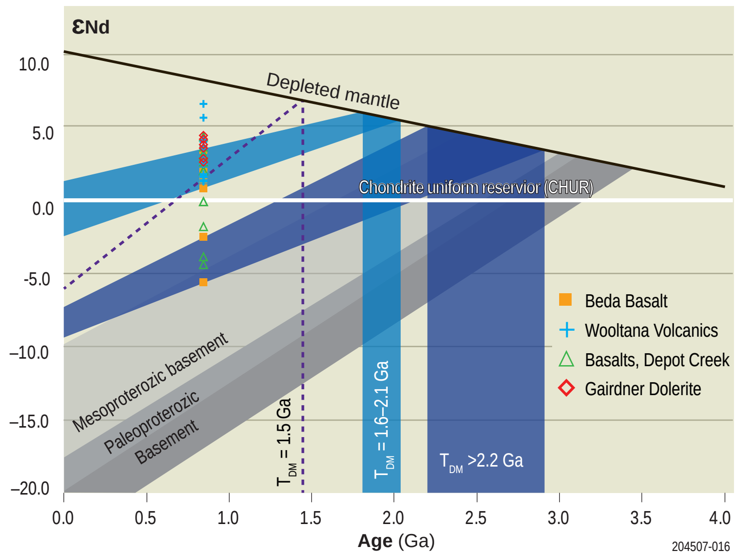


The related large-scale crustal extension and thinning was likely responsible for the formation of the Neoproterozoic Centralian Superbasin in central-southern Australia.

Younger analogues for the Willouran Basic Province include the Cretaceous Paraná-Etendeka large igneous province of South America and southern Africa (Deckart et al. 1998; Ewart et al. 1998), Jurassic Karoo–Ferrar large igneous province of South Africa and Antarctica (Ellam and Cox 1989, 1991; Marzoli et al. 1999; Jourdan et al. 2004) and Miocene–Pliocene Columbia River flood basalts of the western United States (Hooper 1982; Hooper 1990; Hooper 1997). Crawford and Hilyard (1990) demonstrated that the Beda Basalt is a true continental flood tholeiite which displays close affinity to the Paraná basalts. The Wooltana Volcanics display close affinity to tholeiitic basalts erupted immediately prior to the opening of the South Atlantic Ocean.

## Appendix 1: Definition of the Beda Basalt

**Name.** Beda Basalt.

**Derivation of name.** Beda Bore was the first to intersect the basalt.

**Synonyms.** Beda Volcanics (superseded term).

**Lithology.** Subaerial amygdaloidal to massive tholeiitic basalts.

**Age.** Neoproterozoic.

**Distribution.** The Beda Basalt occurs extensively beneath the cover of the younger Neoproterozoic units of the Stuart Shelf in a northwest-trending belt ~190 km by 40 km between the southern tip of the Cultana Inlier and the Carrapateena Arm of Lake Torrens. The only exposure of the formation occurs around the Cultana Inlier, where the basalt is exposed along the coast of the northwestern Spencer Gulf near Backy Point, North and South Hummocks and north of Douglas Point.

**Thickness.** The true thickness of the Beda Basalt is uncertain as it was exposed everywhere to subaerial

*Figure 11 Nd evolution diagrams for the Beda Basalt, Wooltana Volcanics, basalts from Depot Creek and Gairdner Dolerite. $T_{DM}$ age ranges are indicated by dotted line and blue bands.*

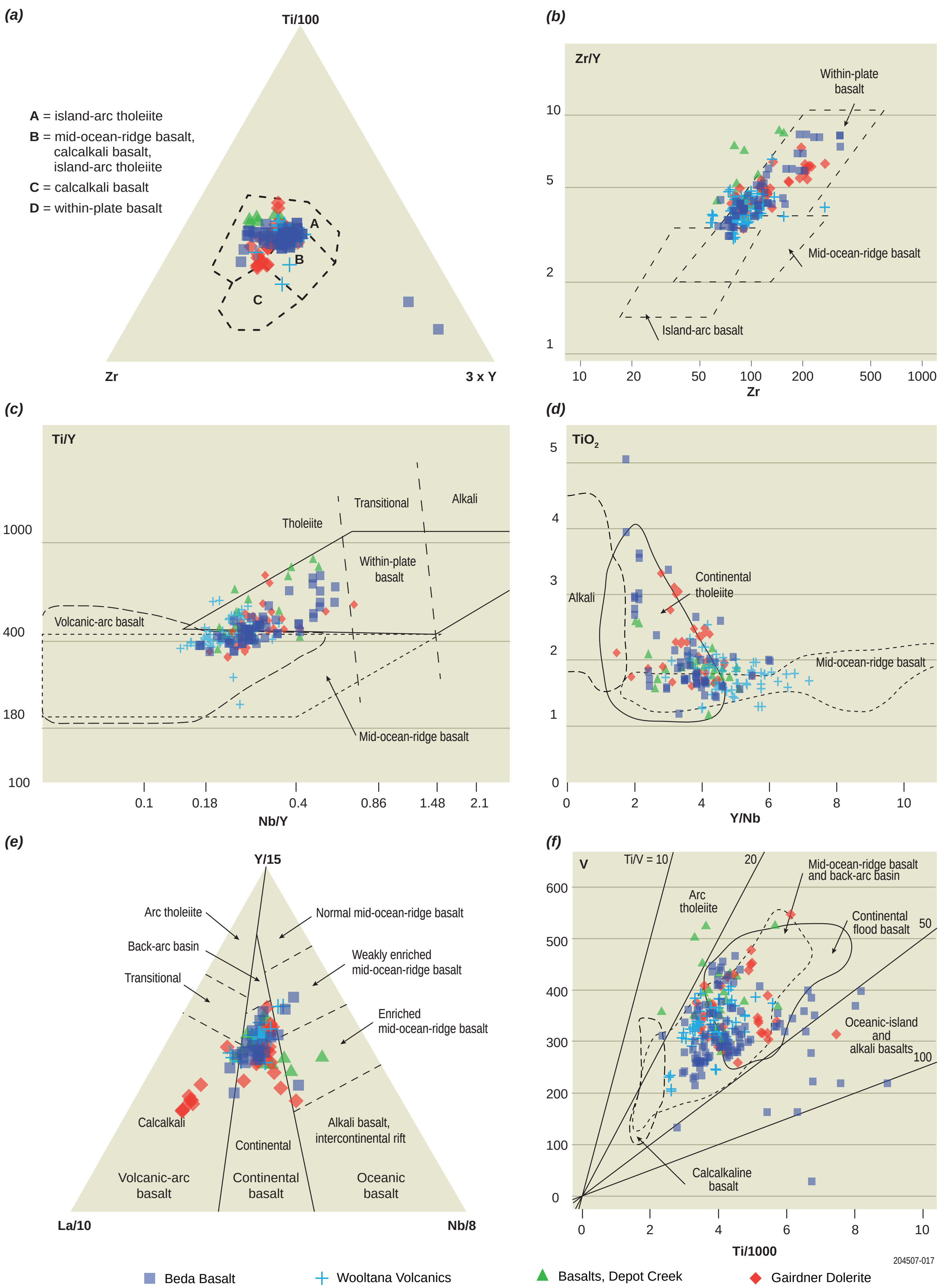


*Figure 12 Tectonic setting discrimination diagrams for the Beda Basalt. (a) Ti–Zr–Y after Pearce and Cann (1973). (b) Zr/Y–Zr after Pearce and Norry (1979). (c) Ti/Y–Nb/Y after Pearce (1982). (d) $TiO_2$–Y/Nb after Floyd and Winchester (1975). (e) Y–La–Nb after Cabanis and Lécolle (1989). (f) V–Ti after Shervais (1982).*

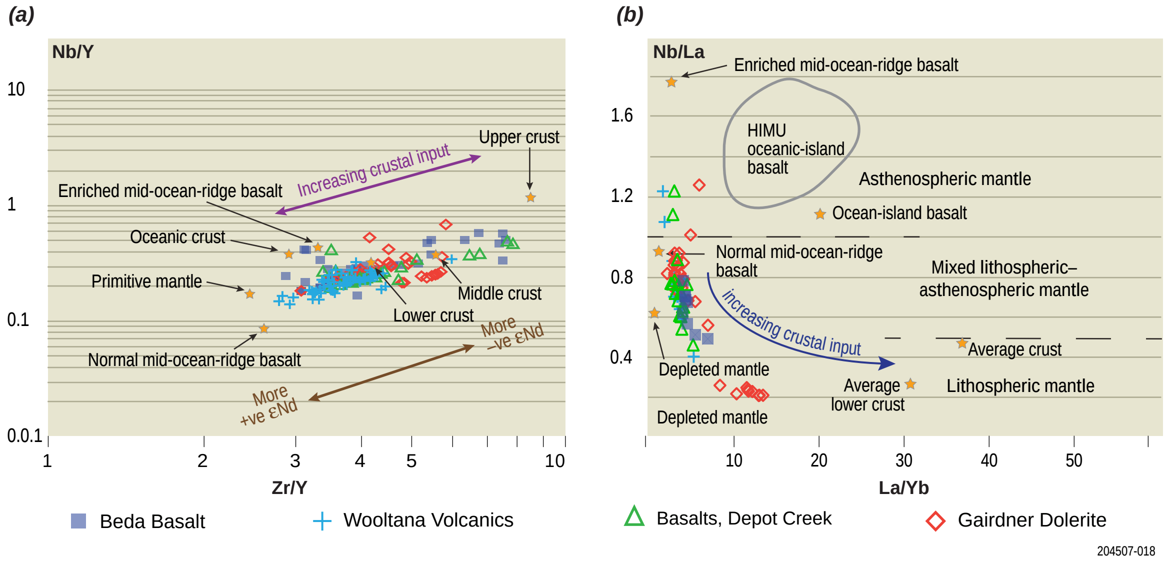


*Figure 13* *Source region discrimination diagrams for the Beda Basalt. (a) Nb/Y–Zr/Y diagram after Fitton et al. (1997). (b) Nb/La–La/Yb diagram after Abdel-Rahman (2002). HIMU = mantle with high U/Pb ratio.*

weathering and erosion prior to the deposition of the Tapley Hill Formation in the early Sturtian. In drillcore, individual flows range in thickness from <1 m to ~30 m thick. In drillhole PSH 1/SAS 1 a pile of 22 lava flows totals almost 200 m thickness.

**Contact relationships.** The Beda Basalt is interlayered with the Backy Point Formation. Small lenses of sand or silt or larger sandstone and conglomerate beds of the Backy Point Formation are recorded between many lava flows in both outcrop (North and South Hummocks, Douglas Point and west of Backy Point) and drillcore (e.g. drillhole TR 3).

Around the Cultana Inlier the Beda Basalt and Backy Point Formation unconformably overlie the Paleoproterozoic (c. 1740 Ma) Moonabie Formation and Mesoproterozoic (c. 1580 Ma) Cultana Subsuite. On the Stuart Shelf they unconformably overlie the Pandurra Formation, and are typically unconformably overlain by the Tapley Hill Formation.

**Type locality and reference drillhole.** The type locality of the Beda Basalt includes exposures around the southeastern Cultana Inlier: Douglas Point (GDA94, zone 53, 762970mE, 6361550mN, extending 400 m to the east and 1.7 km to the north) and 1 km ENE of Backy Point (extending 400 m around the point GDA94, 760060mE, 6354950mN). The interval 273.7–470.44 m from drillhole PSH 1/SAS 1 (DH Number 136943); GDA94, 734729mE, 6409671mN) located 25 km west of Port Augusta, is proposed as the reference drillhole intersection.

## Acknowledgements

The data presented here was compiled from Hörr (1977), Woodget (1987), Crawford and Hilyard (1990), Zhao, McCulloch and Korsch (1994), Foden et al. (2002), Wang et al. (2010) and SA Geodata. New data presented for the Beda Basalt was collected as part of the PORT AUGUSTA mapping program. David Bruce, University of Adelaide, is thanked for assistance with Sm–Nd isotope analysis. John Foden, University of Adelaide, and Wayne Cowley, Geological Survey of South Australia, are thanked for their constructive and careful reviews.

## References

Abdel-Rahman A-FM 2002. Mesozoic volcanism in the Middle East: geochemical, isotopic and petrogenetic evolution of extension-related alkali basalts from central Lebanon. *Geological Magazine* 139(6):621–640.

Australian Selection Pty Ltd 1977. Uro Bluff, progress reports for the period 16/4/75 to 15/3/77, Open File Envelope 02585. Department for Manufacturing, Innovation, Trade, Resources and Energy, South Australia, Adelaide.

Cabanis B and Lécolle M 1989. Le diagramme La/10, Y/15, Nb/8: un outil pour la discrimination des séries volcaniques et la mise en évidence des processus de mélanges et/ou de contamination crustale. *Comptes Rendus de l'Académie des Sciences – Series II* 309:2023–2029.

Compston W, Crawford AR and Bofinger VM 1966. A radiometric estimate of the duration of sedimentation in the Adelaide Geosyncline, South Australia. *Journal of the Geological Society of Australia* 13:229–276.

Cowley WM 1991. *Beda Volcanics and Backy Point Formation of the eastern Gawler Craton*, Report Book 90/16. Department of Mines and Energy South Australia, Adelaide.

Cowley WM and Flint RB 1993. Epicratonic igneous rocks and sediments. In JF Drexel, WV Preiss and AJ Parker eds, *The geology of South Australia, Volume 1, The Precambrian*, Bulletin 54. Geological Survey of South Australia, Adelaide, pp. 142–147.

Crawford AJ and Hilyard D 1990. Geochemistry of late Proterozoic tholeiitic flood basalts, Adelaide Geosyncline, South Australia. In JB Jago and PS Moore eds, *The evolution of a late Precambrian-early Palaeozoic rift complex: the Adelaide Geosyncline*, Special Publication 16. Geological Society of Australia, pp. 49–67.

Crawford AR and Forbes BG 1969. *The geology of the Cultana 1:63 360 map area*, Report of Investigations 34. South Australia Department of Mines, Adelaide.

Crawford AR and Hiern MN 1964. *Cultana*, South Australia, 1:63 360 Geological Atlas Series Map. Geological Survey of South Australia, Adelaide.

Dalgarno CR, Johnson JE, Forbes BG and Thomson BP 1968. *PORT AUGUSTA*, South Australia, 1:250 000 Geological Atlas Series Map, sheet SI53-4. Geological Survey of South Australia, Adelaide.

Deckart K, Féraud GS, Marques L and Bertrand H 1998. New time constraints on dyke swarms related to the Paraná-Etendeka Magmatic Province, and subsequent south Atlantic opening, southeastern Brazil. *Journal of Volcanology and Geothermal Research* 80(1–2):67–83.

Delhi Petroleum Pty Ltd, Urangesellschaft Australia Pty Ltd and CSR Ltd 1986. EL 582 and EL 973, Port Augusta - Lake Torrens area, Open File Envelope 03769. Department for Manufacturing, Innovation, Trade, Resources and Energy, South Australia, Adelaide, pp. 310–314.

Ellam RM and Cox KG 1989. A Proterozoic lithospheric source for Karoo magmatism: evidence from the Nuanetsi Picrites. *Earth and Planetary Science Letters* 92(2):207–218.

Ellam RM and Cox KG 1991. An interpretation of Karoo picrite basalts in terms of interaction between asthenospheric magmas and the mantle lithosphere. *Earth and Planetary Science Letters* 105(1–3):330–342.

Ewart A, Milner SC, Armstrong RA and Dungan AR 1998. Etendeka volcanism of the Goboboseb Mountains and Messum Igneous Complex, Namibia. Part I: Geochemical evidence of Early Cretaceous Tristan Plume melts and the role of crustal contamination in the Paraná–Etendeka CFB. *Journal of Petrology* 39(2):191–225.

Fanning CM, Flint RB and Preiss WV 1983. Geochronology of the Pandurra Formation. *Quarterly Geological Notes* 88:11–16. Geological Survey of South Australia, Adelaide.

Fanning CM, Ludwig KR, Forbes BG and Preiss WV 1986. Single and multigrain U-Pb zircon analyses for the Early Adelaidean Rook Tuff, Willouran Ranges, South Australia. *8th Australian Geological Convention*, pp. 71–72.

Fitton JG, Saunders AD, Norry MJ, Hardarson BS and Taylor RN 1997. Thermal and chemical structure of the Iceland Plume. *Earth and Planetary Science Letters* 153(3–4):197–208.

Floyd PA and Winchester JA 1975. Magma type and tectonic setting discrimination using immobile elements. *Earth and Planetary Science Letters* 27(2):211–218.

Floyd PA and Winchester JA 1978. Identification and discrimination of altered and metamorphosed volcanic rocks using immobile elements. *Chemical Geology* 21:291–306.

Foden J, Song SH, Turner S, Elburg M, Smith PB, van der Steldt B and van Penglis D 2002. Geochemical evolution of lithospheric mantle beneath S.E. South Australia. *Chemical Geology* 182(2–4)663–695.

Fraser GL and Neumann N 2010. *New shrimp U-Pb zircon ages from the Gawler Craton and Curnamona Province, South Australia, 2008-2010*, Record 2010/16. Geoscience Australia, Canberra.

Giles CW and Teale GS 1979. A comparison of the geochemistry of the Roopena Volcanics and the Beda Volcanics. *Quarterly Geological Notes* 71:7–13. Geological Survey of South Australia, Adelaide.

Gordon GA, McAvaney SO, Wade CE and Keeling JL 2014. Characterisation of flows in the Beda Basalt using infrared hyperspectral data. *MESA Journal* 73:42–47. Department of State Development, Adelaide.

Hart SR, Blusztajn J, Dick HJB, Meyer PS and Muehlenbachs K 1999. The fingerprint of seawater circulation in a 500-meter section of ocean crust gabbros. *Geochimica et Cosmochimica Acta* 63:4059–4080.

Hilyard D 1989. Willouran Basic Province: stratigraphy of the late Proterozoic flood basalts, Adelaide Geosyncline, South Australia. In JB Jago and PS Moore eds, *The evolution of a late Precambrian-early Palaeozoic rift complex: the Adelaide Geosyncline*, Special Publication 16. Geological Society of Australia.

Hooper PR 1982. The Columbia River basalts. *Science* 215(4539):1463–1468.

Hooper PR 1990. The timing of crustal extension and the eruption of continental flood basalts. *Nature* 345(246–249).

Hooper PR 1997. The Columbia River Flood Basalt Province: current status. In JJ Mahoney and MF Coffin eds, *Large igneous provinces: continental, oceanic, and planetary flood volcanism*, Geophysical Monograph Series 100. American Geophysical Union, pp. 1–27.

Hörr GM 1977. Precambrian spilites and the Pandurra Formation of the Stuart Shelf, near Port Augusta, South Australia. BSc Hons thesis, University of Adelaide.

Jensen LS 1976. *A new cation plot for classifying subalkalic volcanic rocks*, Miscellaneous Paper 66. Ontario Division of Mines, Toronto.

Johnson JP 1993. The geochronology and radiogenic isotope systematics of the Olympic Dam copper-uranium-gold-silver deposit, South Australia. PhD thesis, Australian National University, Canberra.

Jourdan F, Féraud G, Bertrand H, Kampunzu AB, Tshoso G, Le Gall B, Tiercelin JJ and Capiez P 2004. The Karoo Triple Junction questioned: evidence from Jurassic and Proterozoic $^{40}Ar/^{39}Ar$ ages and geochemistry of the giant Okavango Dyke Swarm (Botswana). *Earth and Planetary Science Letters* 222(3–4):989–1006.

Kendall B, Creaser RA and Selby D 2006. Re-Os geochronology of postglacial black shales in Australia: constraints on the timing of "Sturtian" glaciation. *Geology* 34:729–732.

Klein EM 2004. Geochemistry of the igneous oceanic crust. In RL Rudnick ed., *The crust,* Treatise on Geochemistry 3. Elsevier, pp. 433–463.

Kuno H 1968. Differentiation of basalt magmas. In HH Hess and A Poldervaart eds, *Basalts: the Poldervaart treatise on rocks of basaltic composition, Volume 2*. Interscience Publishers, New York, pp. 632–688.

Le Maitre RW, Bateman P, Dudek A, Keller J, Lameyre J, Le Bas M, Sabine PA, Schmid R, Sorensen H, Streckeisen A, Wooley AR and Zanettin B 1989. *A classification of igneous rocks and glossary of terms*. Blackwell, Oxford.

Li ZX, Li XH, Kinny PD and Wang J 1999. The breakup of Rodinia: did it start with a mantle plume beneath south China? *Earth and Planetary Science Letters* 173:171–181.

Marzoli A, Renne PR, Piccirillo EM, Ernesto M, Bellieni G and Min AD 1999. Extensive 200-million-year-old continental flood basalts of the central Atlantic Magmatic Province. *Science* 284(5414):616–618.

Mason MG, Thomson BP and Tonkin DG 1978. Regional stratigraphy of the Beda Volcanics, Backy Point Beds and Pandurra Formation on the Southern Stuart Shelf, South Australia. *Quarterly Geological Notes* 66:2–9. Geological Survey of South Australia, Adelaide.

McAvaney S 2009. Definition of the Cultana Subsuite: a high-level felsic Hiltaba Suite age intrusive in the eastern Gawler Craton. *MESA Journal* 53:17–27. Department of Primary Industries and Resources South Australia, Adelaide.

Page RW, McCulloch MT and Black LP 1984. Isotopic record of major Precambrian events in Australia. *27th International Geological Congress*, pp. 25–72.

Pearce J and Norry M 1979. Petrogenetic implications of Ti, Zr, Y, and Nb variations in volcanic rocks. *Contributions to Mineralogy and Petrology* 69(1):33–47.

Pearce JA 1982. Trace element characteristics of lavas from destructive plate boundaries. In RS Thorpe ed., *Orogenic andesites and related rocks*. John Wiley and Sons, pp. 528–548.

Pearce JA and Cann JR 1973. Tectonic setting of basic volcanic rocks determined using trace element analyses. *Earth and Planetary Science Letters* 19(2):290–300.

Preiss WV 1987. *The Adelaide Geosyncline: late Proterozoic stratigraphy, sedimentation, palaeontology and tectonics*, Bulletin 53. Geological Survey of South Australia, Adelaide.

Preiss WV 2000. The Adelaide Geosyncline of South Australia and its significance in Neoproterozoic continental reconstruction. *Precambrian Research* 100:21–63.

Rudnick RL and Gao S 2003. Composition of the continental crust. In RL Rudnick ed., *The crust*, Treatise on Geochemistry 3. Elsevier, pp. 1–64.

Shervais JW 1982. Ti-V plots and the petrogenesis of modern and ophiolitic lavas. *Earth and Planetary Science Letters* 59(1):101–118.

Sun, S-s and McDonough WF 1989. *Chemical and isotopic systematics of oceanic basalts: implications for mantle composition and processes,* Special Publications 42:313–345. Geological Society, London.

Wang XC, Li XH, Li ZX and Liu Y 2010. The Willouran Basic Province of South Australia: its relation to the Guibei large igneous province in south China and the breakup of Rodinia. *Lithos* 119:569–584.

Webb AW and Coats RP 1980. *A reassessment of the age of the Beda Volcanics on the Stuart Shelf, South Australia*, Report Book 80/00006. South Australia Department of Mines and Energy, Adelaide.

Webb AW and Hörr G 1978. The Rb-Sr age and petrology of a flow from the Beda Volcanics. *Quarterly Geological Notes* 66:10–13. Geological Survey of South Australia, Adelaide.

Wingate MTD, Campbell IH, Compston W and Gibson GM 1998. Ion microprobe U-Pb ages for Neoproterozoic basaltic magmatism in south-central Australia and implications for the breakup of Rodinia. *Precambrian Research* 87:135–159.

Woodget AL 1987. The petrology, geochemistry and tectonic setting of basic volcanics on the Stuart Shelf and in the Adelaide Geosyncline. Bsc Hons thesis, University of Adelaide.

Zhao J-X, McCulloch MT and Korsch RJ 1994. Characterisation of a plume-related ~800 Ma magmatic event and its implications for basin formation in central-southern Australia. *Earth and Planetary Science Letters* 121:349–367.

FURTHER INFORMATION
**Claire Wade**
Claire.Wade@sa.gov.au
+61 8 8463 3084